Biomechanical Modeling of Cesarean Section Scars and Scar Defects

Adrienne K. Scott[1], Erin M. Louwagie[2] Kristin M. Myers[2], and Michelle L. Oyen[1]

[1] Department of Biomedical Engineering, Washington University in St. Louis, St. Louis MO 63130, USA
sadrienne@wustl.edu
[2] Department of Mechanical Engineering, Columbia University, New York NY 10027, USA

Abstract. Uterine rupture is an intrinsically biomechanical process associated with high maternal and fetal mortality. A previous Cesarean section (C-section) is the main risk factor for uterine rupture in a subsequent pregnancy due to tissue failure at the scar region. Finite element modeling of the uterus and scar tissue presents a promising method to further understand and predict uterine ruptures. Using patient dimensions of an at-term uterus, a C-section scar was modeled with an applied intrauterine pressure to study how scars affect uterine stress. The scar positioning and uterine thickness were varied, and a thickness defect was incorporated into the scar region. The modeled stress distributions confirmed clinical observations as the increased regions of stress due to scar positioning, thinning of the uterine walls, and the presence of a defect are consistent with clinical observations of features that increase the risk of uterine rupture.

Keywords: Cesarean section, uterine rupture, uterine scar, scar defect, finite element modeling

1 Introduction

The current global Cesarean section (C-section) rate is about 21% and is increasing worldwide, especially in developing countries [1, 2]. C-sections are a major abdominal surgery requiring months of recovery time for patients and adding substantial costs to the healthcare system [2, 3]. Although C-sections are essential for decreasing maternal, neonatal, and infant mortality rates, this major surgical procedure can sometimes be performed unnecessarily [4]. In fact, the World Health Organization reports that C-section delivery rates above $10 - 15\%$ are not justified to reduce mortality [5, 6]. Therefore, there is a need to limit the overuse of C-sections and the associated short and longterm complications resulting from this surgery [5].

One inevitable result of a C-section is uterine scarring from the C-section incision. Additionally, inadequate healing of C-section scars can lead to defects

in the scar tissue, also known as an isthmocele or niche [6]. Both the scar and scar defects can lead to a loss of tissue mechanical integrity in a subsequent pregnancy resulting in an increased risk of uterine tissue failure known as uterine rupture or uterine dehiscence: uterine rupture is a complete division of the three tissue layers in the uterus (perimetrium, myometrium, and endometrium), while uterine dehiscence is only a partial division of the uterine layers [7]. In a subsequent pregnancy after a C-section the rate of uterine rupture increases to approximately 0.5% [8]. In comparison, the rate of uterine rupture is only about 0.02% in patients with no prior C-section [9]. Although a rate of 0.5% is low, uterine rupture is a life-threatening emergency as neonatal mortality ranges from 74 to 94% and maternal mortality ranges from 1 to 13 % due to uterine rupture [10].

To prevent uterine rupture, it is important to consider all of the associated risk factors in addition to the presence of a scar and scar defects. Clinical data has shown that the positioning of the scar alone influences the risk of uterine rupture. Historically, the first classical C-section incisions were vertical along the sagittal plane. Now, it is well known that vertical scars in the uterus further increase the risk of uterine rupture [11]. For this reason, vertical incisions are avoided unless needed for emergencies, and low transverse incisions are used instead. Recent literature has also shown how uterine structure, such as thinning of the lower uterine segment measured by 2D ultrasound, correlates to uterine rupture risk [12, 13]. Additionally, connective tissue disorders that are likely to affect the mechanical properties of the tissue are also associated with an increased risk of uterine rupture [14]. Taken as a whole, it is evident that uterine rupture is a mechanical process that could be evaluated using engineering tools.

Although some risk factors have been identified, there is currently no reliable model to predict uterine rupture. Furthermore, to our knowledge, no one has previously examined the risk of uterine rupture with C-section scars with a biomechanical approach. Finite element (FE) modeling of the uterus and the scar tissue may present a promising method to further understand and predict uterine ruptures. FE models allow for the study of how various parameters (patient geometry, mechanical properties) influence uterine mechanics. Therefore, our objective is to generate a mechanical model of the uterus to examine how the scar positioning (sagittal versus transverse), material properties of the scar, and the presence of a defect influence uterine tissue mechanics.

2 Methods

Parametric Geometries A baseline representative model of a uterus and cervix was generated by averaging patient uterine dimensions acquired from MRI images of five at-term pregnant patients and constructing a geometry in Solidworks 2022 (Dassault Systémes, France) as previously described [15–17]. A scar (Fig. 1A) and surrounding abdomen tissue were also included in the Solidworks model [18]. The scar was split into two parts to allow variance of the material properties at the midline of both the transverse and sagittal scar (Fig.

1B). The standard deviation of four uterine thickness measurements (fundal, anterior, left/right, and lower uterine segment thickness, or UT1, UT2, UT3, UT4 respectively) of the five at-term pregnant patients were calculated and added or subtracted from the average baseline model (Fig. 1C). Geometries were then built in Solidworks to vary the uterine thickness by increasing the thickness values by a standard deviation (baseline + SD) and decreasing the thickness values by a standard deviation (baseline – SD) (Fig. 1C). Next, a defect was incorporated in to the scar tissue (Fig. 1D). Dimensions of the defect size (i.e., width, depth, length) were based on average measurements found in the literature [20, 19].

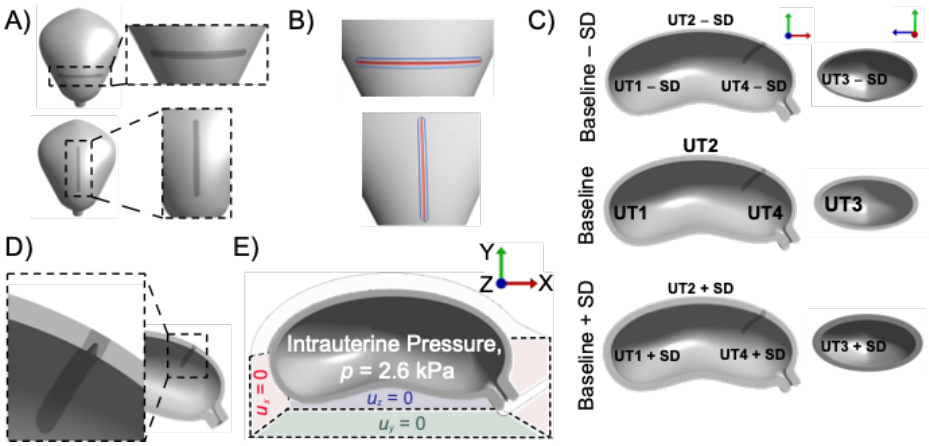

Fig. 1. A) Representative baseline models of a uterus and cervix with sagittal and transverse C-section scars were generated from measurements acquired from MRI images of at-term pregnant patients. B) The scar geometry was split through the midline so that the stiffness (E) of the midline could be varied, and the remaining stiffness was linearly interpolated to the surrounding uterine stiffness. C) The uterine thickness was varied by increasing and decreasing the fundal (UT1), anterior (UT2), left/right (UT3) and lower uterine segment (UT4) thickness by a standard deviation (SD) of patient measurements. D) A defect was incorporated in the model with a low transverse scar. E) The displacement of the abdomen walls was fixed in the x, y and z directions and an intrauterine pressure was applied (p = 2.6 kPa).

Mesh Generation The abdomen, uterus, cervix, and scar geometries with and without defects were discretized into linear tetrahedral elements using Hypermesh 2022 (Altair, Michigan, U.S.A.). The element sizes were determined through a mesh convergence study to determine when the von Mises stress values (σ) of specified nodes in the uterus and scar geometries converged to a solution.

Finite Element Simulation and Analysis Meshed geometries were imported into FEBio Studio (v2.2) and modeled as a nearly incompressible (Poisson's ratio

$\nu = 0.48$) neo-Hookean material according to the FEBio manual [21, 22]. The Young's modulus (E) of the abdomen and the uterus were set to 100 kPa, while the stiffness of the scar tissue was varied. First, the scar tissue was treated as a homogeneous material and the Young's modulus (E) of the scar was varied (50 kPa, 100 kPa, 200 kPa). Next, the Young's modulus of the midline of the scar region was varied (50 kPa, 100 kPa, 200 kPa). The Young's modulus of the remaining scar tissue was calculated by a linear interpolation between the midline value and the surrounding uterine tissue. Displacement of the abdomen walls in the x, y and z directions were fixed and a physiological intrauterine pressure ($p = 2.6$ kPa) was applied as shown in Fig. 1E [23]. The models were performed and analyzed using FEBio (v4.2) and FEBio Studio (v2.2). The von Mises stress was calculated as described in the FEBio Manual [24].

3 Results

To understand how the presence of a sagittal scar instead of a low transverse scar could increase the risk of uterine rupture, the von Mises stress on the scar region of both types of scars were compared. Heat maps of von Mises stress revealed that stress on the anterior side of the sagittal scar is greater than that on the anterior side of the transverse scar (Fig. 2A). The models in which the scar properties matched the surrounding tissue properties validated the boundary conditions and demonstrated the expected null-response. Additionally, varying the stiffness of the scar region from 50 kPa to 200 kPa showed that as the scar stiffness increases, so does the stress in the scar region, as expected (Fig. 2A). Plotting the von Mises stress in the scar region as a histogram normalized to element volume confirmed that the maximum stress was greater in the sagittal scar compared to the respective transverse scar with the same Young's modulus (Fig. 2B). Next, the stiffness of the midline of the scar was varied to allow for a gradient change in stiffness to the scar midline. In this case, the results were similar to the homogeneous scars (Fig. 3).

Since the thickness of the lower uterine segment has been shown to be predictive of uterine rupture, the thickness of the uterine tissue was also varied. When varying the thickness of the uterine wall, heat maps of the von Mises stress in the scar region showed that decreasing the wall thickness increased the stress in the scar region (Fig. 4). Plotting the calculated stress values of each element in the scar region as a histogram normalized to element volume confirmed that the mean and maximum stress does increase with decreasing thickness (Fig. 4).

Incorporating a defect in the low transverse scar caused stress concentrations in the posterior side of the defect region (Fig. 5A). Quantifying the stress along the midline of the scar from the outer edge to the center demonstrated that there is an increase in von Mises stress at the defect region compared to the model with no defect incorporated (Fig. 5B).

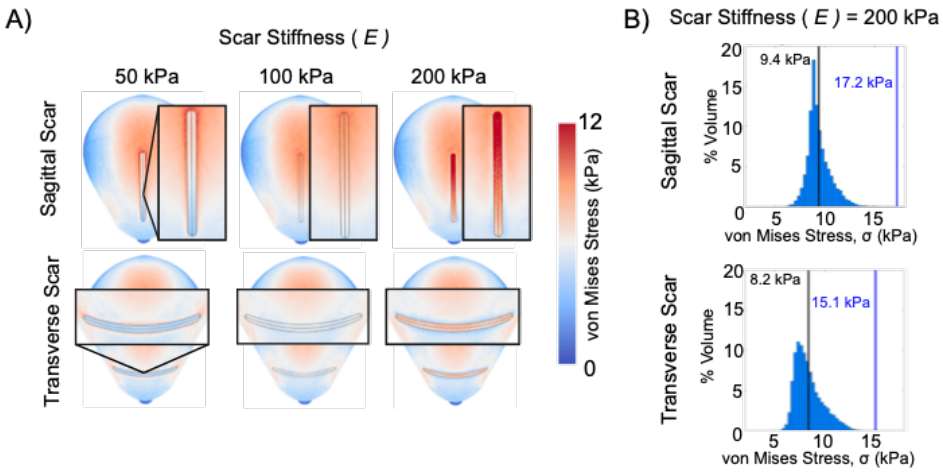

Fig. 2. A) Heat maps of von Mises stress (σ) were generated and showed increased stress with sagittal scars compared to transverse scars with the same stiffness (E). B) The average (black line) and maximum (blue line) von Mises stress in the scar region of the sagittal scar was greater compared to the transverse scar with the same stiffness ($E = 200$ kPa).

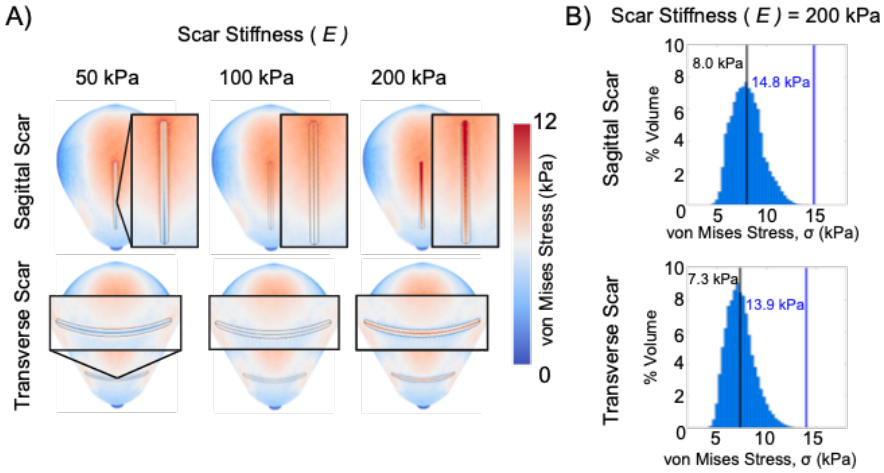

Fig. 3. A) The stiffness (E) of the midline of the scar was varied, which allowed for a gradient of stiffness between the surrounding uterine tissue. Von Mises stress (σ) distributions show similar trends to the homogeneous scars. B) The average (black line) and maximum (blue line) von Mises stress in the scar region of the sagittal scar was greater compared to the transverse scar with the same stiffness ($E = 200$ kPa).

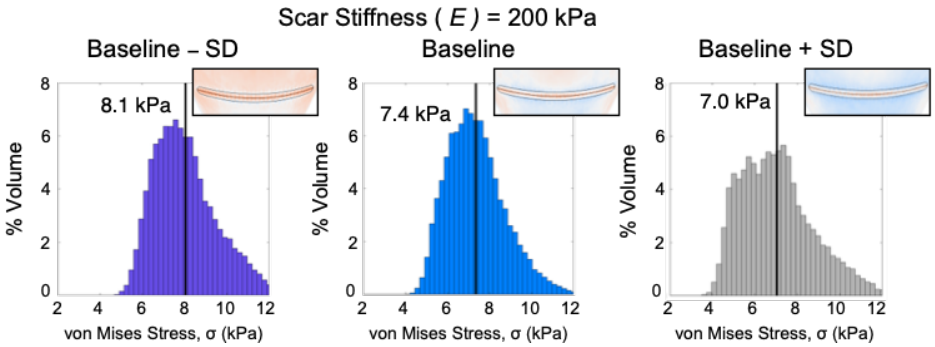

Fig. 4. The uterine thickness was increased and decreased by the standard deviation (SD) of five patients' uterine thickness measurements and the scar stiffness was held constant ($E = 200$ kPa). The mean von Mises stress (σ) in the scar region decreased with increasing uterine thickness.

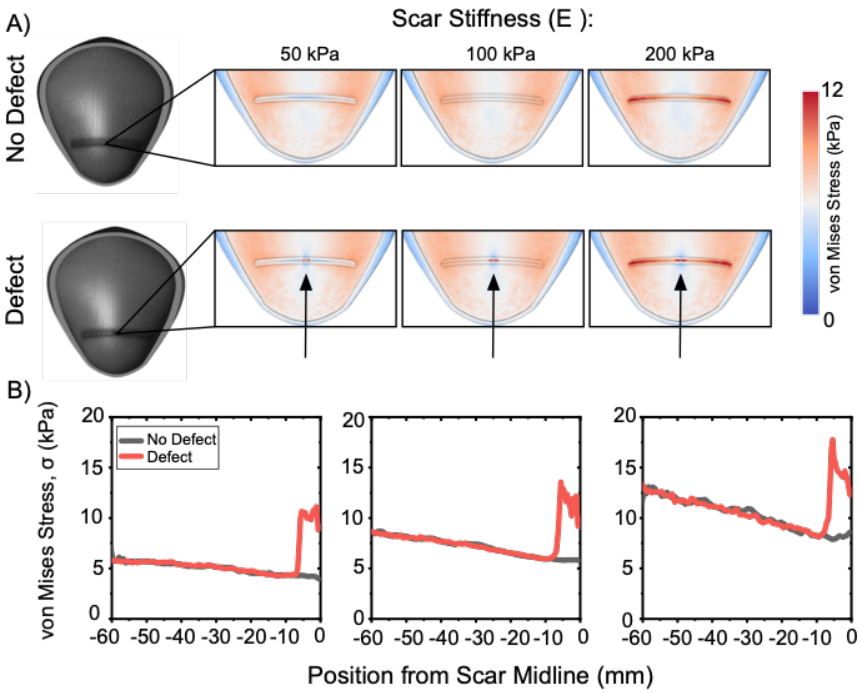

Fig. 5. A) Compared to the models with no scar defect, the von Mises stress in the interior of the defect region increases. The stress on the defect also increases with increasing scar stiffness, as expected. B) Plotting the von Mises stress of elements along the edge of the scar from the outer edge (–60 mm) to the center of the scar in the defect region (0 mm) demonstrates the increased stress in the defect region.

4 Discussion

In conclusion, scar positioning, decreasing uterine thickness, and the presence of a defect are all factors that increase the stress in the scar region, suggesting the tissue may be more likely to fail in this location. Taken together, the results of this proof-of-concept study are promising because the increased regions of stress due to scar positioning, thinning of the uterine walls and the presence of a defect are consistent with clinical observations of features that increase the risk of uterine rupture. While the results are promising, this work includes several limitations. The model assumes all tissues can be represented as a neo-Hookean material, but other materials, such as a fibrous material, may be more representative of the uterine and scar tissue [25, 26]. Additionally, we chose a Young's modulus range of 50 – 200 kPa, but in the future more accurate measurements of material properties of uterine tissue could be incorporated into the model. This model also did not account for spatial variation of material properties in the uterine tissue. While there was a spatial variation of material properties of the scar tissue, we assumed that the greatest change in the elastic modulus was at the midline of the scar tissue, which may not accurately represent the spatial variation of material properties in C-sections scars. Therefore, future work is needed to characterize the material properties and spatial variation of material properties of uterine tissue and C-section scars.

Overall, this study demonstrates a framework to build patient specific geometries of C-section scars and scar defects to understand how these structures influence uterine deformation and stress under an applied load. In the future, further parametric models could identify critical parameters that influence uterine rupture risk and perhaps identify new assessments of risk that can be considered for patient specific surgical planning.

Acknowledgements. The authors acknowledge the NIH T32 Postdoctoral Training Grant in Regenerative Medicine (T32 EB028092).

References

1. Betrán, A. P., Ye, J., Moller, A. B., Zhang, J., Gülmezoglu, A. M., and Torloni, M. R.: The increasing trend in caesarean section rates: global, regional and national estimates: 1990-2014. Plos One. 11(2), e0148343 (2016). https://doi.org/10.1371/journal.pone.0148343
2. Betrán, A. P., Ye, J., Moller, A. B., Souza, J. P., and Zhang, J.: Trends and projections of caesarean section rates: global and regional estimates. BMJ Global Health, 6(6), e005671 (2021). https://doi.org/10.1136/bmjgh-2021-005671
3. Hoxha, I., and Fink, G.: Caesarean sections and health financing: a global analysis. BMJ Open, 11(5), e044383 (2021). https://doi.org/10.1136/bmjopen-2020-044383
4. Sobhy, S., Arroyo-Manzano, D., Murugesu, N., Karthikeyan, G., Kumar, V., Kaur, I., ... and Thangaratinam, S.: Maternal and perinatal mortality and complications associated with caesarean section in low-income and middle-income countries: a systematic review and meta-analysis. The Lancet, 393(10184), 1973-1982 (2019). https://doi.org/10.1136/bmjopen-2020-044383

5. Betrán, A. P., Torloni, M. R., Zhang, J., Ye, J., Mikolajczyk, R., Deneux-Tharaux, C., ... and Gülmezoglu, A. M.: What is the optimal rate of caesarean section at population level? A systematic review of ecologic studies. Reproductive Health, 12(1), 1-10 (2015). https://doi.org/10.1186/s12978-015-0043-6
6. Antila-Långsjö, R. M., Mäenpää, J. U., Huhtala, H. S., Tomás, E. I., and Staff, S. M.: Cesarean scar defect: a prospective study on risk factors. American Journal of Obstetrics and Gynecology, 219(5), 458-e1 (2018). https://doi.org/10.1016/j.ajog.2018.09.004
7. Zhu, Z., Li, H., and Zhang, J.: Uterine dehiscence in pregnant with previous caesarean delivery. Annals of Medicine, 53(1), 1266-1270 (2021). https://doi.org/10.1080/07853890.2021.1959049
8. Motomura, K., Ganchimeg, T., Nagata, C., Ota, E., Vogel, J. P., Betran, A. P., ... and Mori, R.: Incidence and outcomes of uterine rupture among women with prior caesarean section: WHO Multicountry Survey on Maternal and Newborn Health. Scientific Reports, 7(1), 44093 (2017). https://doi.org/10.1038/srep44093
9. Dow, M., Wax, J. R., Pinette, M. G., Blackstone, J., and Cartin, A.: Third-trimester uterine rupture without previous cesarean: a case series and review of the literature. American Journal of Perinatology, 26(10), 739-744 (2009). https://doi.org/10.1055/s-0029-1223287
10. Justus Hofmeyr, G., Say, L., and Metin Gülmezoglu, A.: Systematic review: WHO systematic review of maternal mortality and morbidity: the prevalence of uterine rupture. BJOG: An International Journal of Obstetrics & Gynaecology, 112(9), 1221-1228 (2005). https://doi.org/10.1111/j.1471-0528.2005.00725.x
11. Landon, M. B., Hauth, J. C., Leveno, K. J., Spong, C. Y., Leindecker, S., Varner, M. W., ... and Gabbe, S. G.: Maternal and perinatal outcomes associated with a trial of labor after prior cesarean delivery. New England Journal of Medicine, 351(25), 2581-2589 (2004). https://doi.org/10.1016/j.jmwh.2005.06.001
12. Rozenberg, P., Sénat, M. V., Deruelle, P., Winer, N., Simon, E., Ville, Y., ... and Groupe de Recherche en Obstétrique et Gynécologie.: Evaluation of the usefulness of ultrasound measurement of the lower uterine segment before delivery of women with a prior cesarean delivery: a randomized trial. American Journal of Obstetrics & Gynecology, 226(2), 253-e1 (2022). https://doi.org/10.1016/j.ajog.2021.08.005
13. Bujold, E., Jastrow, N., Simoneau, J., Brunet, S., and Gauthier, R. J.: Prediction of complete uterine rupture by sonographic evaluation of the lower uterine segment. American Journal of Obstetrics & Gynecology, 201(3), 320-e1 (2009). https://doi.org/10.1016/j.ajog.2009.06.014
14. Aboughalia, H., Basavalingu, D., Revzin, M. V., Sienas, L. E., Katz, D. S., and Moshiri, M.: Imaging evaluation of uterine perforation and rupture. Abdominal Radiology, 46(10), 4946-4966 (2021). https://doi.org/10.1007/s00261-021-03171-z
15. Louwagie, E. M., Carlson, L., Over, V., Mao, L., Fang, S., Westervelt, A., ... and Myers, K.: Longitudinal ultrasonic dimensions and parametric solid models of the gravid uterus and cervix. Plos One, 16(1), e0242118 (2021). https://doi.org/10.1371/journal.pone.0242118
16. Rajasekharan, D., Feder, A. D., Louwagie, E. M., and Myers, K. M.: Summer 2020 Undergrad Project-Late Pregnancy Uterus Model. (2020). https://doi.org/10.7916/d8-p164-vg61
17. Joyce, E. M., Diaz, P., Tamarkin, S., Moore, R., Strohl, A., Stetzer, B., ... and Moore, J. J.: In-vivo stretch of term human fetal membranes. Placenta, 38, 57-66 (2016). https://doi.org/10.1016/j.placenta.2015.12.011
18. Kan, A.: Classical cesarean section. The Surgery Journal, 6(S 02), S98-S103 (2020). https://doi.org/10.1055/s-0039-3402072

19. Naji, O., Abdallah, Y., Bij De Vaate, A. J., Smith, A., Pexsters, A., Stalder, C., ... and Bourne, T.: Standardized approach for imaging and measuring Cesarean section scars using ultrasonography. Ultrasound in Obstetrics & Gynecology, 39(3), 252-259 (2012). https://doi.org/10.1002/uog.10077
20. Savukyne, E., Machtejeviene, E., Paskauskas, S., Ramoniene, G., and Nadisauskiene, R. J.: Transvaginal sonographic evaluation of cesarean section scar niche in pregnancy: a prospective longitudinal study. Medicina, 57(10), 1091 (2021). https://doi.org/10.3390/medicina57101091
21. Maas, S. A., Ellis, B. J., Ateshian, G. A., and Weiss, J. A.: FEBio: finite elements for biomechanics. Journal of Biomechanical Engineering, (2012). https://doi.org/10.1115/1.4005694
22. Maas, S. A., Herron, M., Weiss, J. A., and Ateshian, G. A.: Subsection 5.2.3 of febio theory manual: Neo-hookean hyperelasticity. (2023). https://help.febio.org/FEBioTheory/FEBiotm3-4-Subsection-5.2.3, Last accessed on 2023-06-20.
23. Wheeler, M. L., and Oyen, M. L.: Premature rupture of membranes and severe weather systems. Frontiers in Physiology, 11, 524 (2020). https://doi.org/10.3389/fphys.2020.00524
24. Maas, S. A., Herron, M., Weiss, J. A., and Ateshian, G. A.: Subsection 4.6.3.4 of FEBio Theory Manual: Von Mises Stress. (2023). https://help.febio.org/docs/FEBioUser-3-6/UM36-4.6.3.4, Last accessed on 2023-06-20.
25. Myers, K. M., Hendon, C. P., Gan, Y., Yao, W., Yoshida, K., Fernandez, M., ... and Wapner, R. J.: A continuous fiber distribution material model for human cervical tissue. Journal of Biomechanics, 48(9), 1533-1540 (2015). https://doi.org/10.1016/j.jbiomech.2015.02.060
26. Weiss, S., Jaermann, T., Schmid, P., Staempfli, P., Boesiger, P., Niederer, P., ... and Bajka, M.: Three-dimensional fiber architecture of the nonpregnant human uterus determined ex vivo using magnetic resonance diffusion tensor imaging. The Anatomical Record Part A, 288(1), 84-90 (2006). https://doi.org/10.1002/ar.a.20274